

Engineering *Escherichia coli* membrane phospholipid head distribution improves tolerance and production of biorenewables[☆]



Zaigao Tan^{a,b}, Pouyan Khakbaz^c, Yingxi Chen^{a,b}, Jeremy Lombardo^{b,d}, Jong Moon Yoon^{a,b}, Jacqueline V. Shanks^{a,b}, Jeffery B. Klauda^{c,e}, Laura R. Jarboe^{a,b,*}

^a Department of Chemical and Biological Engineering, Iowa State University, Ames, IA 50011, USA

^b NSF Engineering Research Center for Biorenewable Chemicals, Iowa State University, Ames, IA 50011, USA

^c Department of Chemical and Biomolecular Engineering, University of Maryland, College Park, MD 20742, USA

^d Department of Bioengineering, University of Missouri, Columbia, MO 65211, USA

^e Biophysics Program and the University of Maryland Energy Research Center, University of Maryland, College Park, MD, USA

ARTICLE INFO

Keywords:

Phospholipids
Phosphoethanolamine (PE)
Octanoic acid
Hydrophobic core

ABSTRACT

Economically competitive microbial production of biorenewable fuels and chemicals is often impeded by toxicity of the product to the microbe. Membrane damage is often identified as a major mechanism of this toxicity. Prior efforts to strengthen the microbial membrane by changing the phospholipid distribution have largely focused on the fatty acid tails. Herein, a novel strategy of phospholipid head engineering is demonstrated in *Escherichia coli*. Specifically, increasing the expression of phosphatidylserine synthase (+*pssA*) was found to significantly increase both the tolerance and production of octanoic acid, a representative membrane-damaging solvent. Tolerance of other industrially-relevant inhibitors, such as furfural, acetate, toluene, ethanol and low pH was also increased. In addition to the increase in the relative abundance of the phosphoethanolamine (PE) head group in the +*pssA* strain, there were also changes in the fatty acid tail composition, resulting in an increase in average length, percent unsaturation and decreased abundance of cyclic rings. This +*pssA* strain had significant changes in: membrane integrity, surface potential, electrochemical potential and hydrophobicity; sensitivity to intracellular acidification; and distribution of the phospholipid tails, including an increase in average length and percent unsaturation and decreased abundance of cyclic rings. Molecular dynamics simulations demonstrated that the +PE membrane had increased resistance to penetration of ethanol into the hydrophobic core and also the membrane thickness. Further hybrid models in which only the head group distribution or fatty acid tail distribution was altered showed that the increase in PE content is responsible for the increase in bilayer thickness, but the increased hydrophobic core thickness is due to altered distribution of both the head groups and fatty acid tails. This work demonstrates the importance of consideration of the membrane head groups, as well as a modeling approach, in membrane engineering efforts.

1. Introduction

Construction of microbial cell factories for synthesis of bio-products using cheap and renewable feedstocks is an attractive alternative to current petroleum-based production methods (Larson, 2006; Energy, 2016; Kircher, 2015; Dale, 2011). A variety of microbes have been genetically engineered for production of biofuels, bulk chemicals, and high-value fine chemicals (Zhu et al., 2014; Park et al., 2012; McKenna and Nielsen, 2011; Atsumi et al., 2008; Galanie et al., 2015). Although many high-performing strains have been described, strain performance is often still limited by inhibition of microbial activity by components of

the feedstock and the bio-products (Dunlop et al., 2011; Jarboe et al., 2011; Chen and Dou, 2016).

Arguably, membrane damage has been deemed as a fundamental mechanism of inhibitor toxicity due to the membrane's role as a protective barrier (Lennen et al., 2011; Liu et al., 2013; Royce et al., 2013; Zaldivar and Ingram, 1999). Ethanol was observed to fluidize the cell membrane, leading to leakage of important ions and arbitrary transport of solutes, which decreased the transmembrane potential and proton gradient (Huffer et al., 2011). Transcriptome-based analysis led to the conclusion that membrane damage is a key component of isobutanol toxicity, possibly due to disruption of the electron transport chain

[☆] This work will be included in patent applications by Iowa State University.

* Correspondence to: Department of Chemical and Biological Engineering, 4134 Biorenewables Research Laboratory, Iowa State University, Ames, IA 50011, USA.
E-mail address: ljjarboe@iastate.edu (L.R. Jarboe).

(Brynildsen and Liao, 2009). Both membrane integrity and cell viability decrease markedly during fatty acid production (Lennen et al., 2011). Our prior studies also showed that either exogenously-added or endogenously-produced fatty acids or styrene increased membrane leakage of *E. coli* (Royce et al., 2013; Lian et al., 2016). If one envisions each microbial biocatalyst as a reactor, this membrane damage is analogous to a reaction vessel being corroded by its contents. The standard approach in this scenario would be to change the composition of the vessel so that it is resistant to this damage. This approach can also be applied to the microbial cell membrane (Sandoval and Papoutsakis, 2016), with the goal of increasing tolerance (Lennen and Pfleger, 2013; Luo et al., 2009; Tan et al., 2016; Besada-Lombana et al., 2017) and production (Tan et al., 2016; Sherkhanov et al., 2014) of membrane-damaging compounds.

Fatty acids, which can serve as catalytic precursors for a variety of chemicals (Korstanje et al., 2015), are widely used in production of lubricants, preservatives, and fuels and thus are an attractive fermentation product. However, as stated above, these compounds have also been reported to cause microbial membrane damage during production (Lennen et al., 2011; Royce et al., 2013). The fatty acid tails of the membrane phospholipids have been a previous engineering target, with the intention of alleviating toxicity. For example, increasing the average length of membrane lipids partially alleviated the toxicity of fatty acids and increased fatty acid titers by 20% (Sherkhanov et al., 2014). Altering the relative distribution of the saturated and unsaturated fatty acid tails was effective in alleviating membrane leakage during fatty acid production, although fatty acid production was not increased (Lennen and Pfleger, 2013). Our prior study showed that production of non-native trans unsaturated fatty acids (TUFA) significantly decreased membrane fluidity and increased fatty acid tolerance and production (Tan et al., 2016). This TUFA production in *E. coli* also increased tolerance and production of other membrane-damaging biorenewables (Tan et al., 2016).

These previous results demonstrate that engineering of the length, degree of saturation and conformation of the phospholipid fatty acids can improve tolerance and/or production of membrane-damaging compounds (Lennen and Pfleger, 2013; Luo et al., 2009; Tan et al., 2016; Besada-Lombana et al., 2017; Sherkhanov et al., 2014). However, by focusing on the fatty acids, these studies addressed the tails of the phospholipid molecules, and we know relatively little about the role of the phospholipid head group in tolerance and production of membrane-damaging compounds. Inspired by our previous computational results which indicated that the degree of membrane disruption imposed by ethanol differed according to the phospholipid head group identity (Konas et al., 2015), here we postulated that engineering the phospholipid head group distribution might be an effective strategy for engineering robustness. To this end, a proof-of-concept design was conceived and performed to alter the phospholipid head distribution. Specifically, the abundance of three different phospholipids (phosphatidylethanolamine (PE), phosphatidylglycerol (PG) and cardiolipin (CL)) with distinct head groups was modulated by altering the expression of key phospholipid biosynthesis enzymes PssA, PgsA, and ClsA. While other studies have concluded that alteration of the phospholipid head distribution is detrimental to cellular function and resistance to environmental stressors (Rowlett et al., 2017), here we report that increasing the relative abundance of the PE head group (+PE) increased tolerance and production of representative membrane-damaging short-chain fatty acids and also increased tolerance of the model biomass-derived inhibitors furfural and acetate. Computational analysis of this membrane engineering strategy indicates that this increased tolerance to membrane-damaging compounds is due to decreased penetration of membrane-damaging compounds into the membrane hydrophobic core and increased membrane thickness.

2. Materials and methods

Detailed materials and methods can be found in the online supporting material.

2.1. Strains and plasmids

All plasmids and strains used in this paper are listed in Table S1. All strains are derivatives of *E. coli* MG1655. One-step recombination (FLP-FRT) was used for chromosomal editing (Datsenko and Wanner, 2000). Gene expression was increased by chromosomal insertion of a second gene copy and regulation usually by strong promoter M1-93, or other promoters as specified (Zhu et al., 2014; Tan et al., 2013; Zhang et al., 2009; Lu et al., 2012). Copies of *pssA*, *clsA* and *pgsA* were inserted at *ldhA*; *acrAB* was integrated at *mgsA* site, and *tolC* was integrated at *maeB*. For octanoic acid production, the pJMYEEI82564 plasmid harboring thioesterase of *Anaerococcus tetradium* was used (San et al., 2011).

2.2. Growth conditions and characterization

All tolerance experiments were performed in 250 mL baffled flasks containing 50 mL MOPS with 2.0% (w/v) dextrose (Neidhard et al., 1974) at 220 rpm and initial pH 7.0. Tolerance to octanoic acid was assessed at 30 °C or 37 °C, high temperature tolerance was assessed at 42 °C, all other tolerance experiments were performed at 37 °C. Specific growth rate μ (h^{-1}) was calculated by fitting the equation $\text{OD}_{550,t} = \text{OD}_{550,0}e^{\mu t}$ to the exponential growth phase. All estimated μ values had an R^2 of at least 0.95.

2.3. Membrane and cell surface characterization

Membrane integrity was analyzed by SYTOX green (Invitrogen) staining (Lennen and Pfleger, 2013), membrane fluidity by 1,6-diphenyl-1,3,5-hexatriene (DPH) (Invitrogen) (Royce et al., 2013), membrane surface potential by monovalent cationic fluorescence dye 9-aminoacridine (9-AA) (Carbon and Luna, 1991), and membrane electrochemical potential by DiOC₂(3) dye (Thermo Fisher Scientific). Intracellular pH was measured by pTorA-GFPmut3* (pJDT1) plasmid (Royce et al., 2014). Cellular hydrophobicity was analyzed by addition of n-hexane (Royce et al., 2013). Membrane-bound fatty acids were extracted by a modified Bligh and Dyer method (Bligh and Dyer, 1959) and analyzed by GC-MS (Royce et al., 2013). Phospholipids distribution was analyzed by HPLC-ELSD (Agilent) (Becart et al., 1990).

2.4. Preparation of the corn stover hydrolysate

Corn stover hydrolysate was kindly provided by Nancy Nichols and Sarah Frazer from National Center for Agricultural Utilization Research, U.S. Department of Agriculture. Ten grams of corn stover were milled and passed through a 4 mm screen, mixed with 100 mL of 0.5% (v/v) sulfuric acid and heated to 160 °C for 10 min. The reaction product was filtered and the solids were washed. Calcium hydroxide was added, with stirring, to pH 6.5. The hydrolysate was filtered again and stored at or below 4 °C until use. The hydrolysate composition is given in Table S7.

2.5. Carboxylic acid production

Individual colonies from Luria Broth (LB) plates with ampicillin were inoculated into LB liquid medium with ampicillin and grown for 4 h. Then, 0.5 mL of culture was added to 20 mL MOPS 2.0% dextrose with ampicillin at 30 °C, 220 rpm and grown overnight as seed culture. Fermentations were performed in 50 mL MOPS 2.0% dextrose with ampicillin and an initial pH of 7.0 at an initial OD₅₅₀ of 0.1. Where indicated, furfural, acetate and vanillic acid (FAV) were added at final

concentrations of 0.8, 1.2 and 0.5 g/L, respectively. When OD₅₅₀~0.5, isopropyl-β-D-thiogalactopyranoside (IPTG) was added at a final concentration of 1.0 mM to induce thioesterase expression. Cultures were grown at 30 °C, 220 rpm for 72 or 96 h. Carboxylic acids were extracted from the fermentation broth and quantified by an Agilent 7890 gas chromatograph equipped with an Agilent 5975 mass spectrometer using flame ionization detector and mass spectrometer (GC-FID/MS). C7:0, C11:0, C13:0, C15:0 and C17:0 were used as internal standards.

2.6. MD simulations

Model lipid bilayers contained a total of 160 lipids maintained at 310.15 K and 1 bar. Systems were fully hydrated and the hydration numbers for systems with and without ethanol were specified as 50 and 35, respectively. All-atom molecular dynamics (MD) simulations using explicit solvent were carried out for all systems. Initial membrane conformations were built by CHARMM-GUI *Membrane Builder* (Jo et al., 2007, 2008, 2009; Wu et al., 2014). Minimization, equilibration, and isobaric-isothermal ensemble (NPT) MD simulations were performed using NAMD simulation package. Lennard-Jones potential was used to describe van der Waals interactions, with a force-based switching function in the range of 8–12 Å. After equilibration, each simulation was run for 300 ns using a time step of 2 fs. The Particle Mesh Ewald method was used for long-range electrostatics interactions. Hydrogen atoms were constrained by the RATTLE algorithm. The CHARMM36 (C36) force field was used (Klauda et al., 2010; Pandit and Klauda, 2012). Langevin dynamics maintained the temperature and the Nosé–Hoover Langevin-piston algorithm was used to maintain the pressure. Three replicates were carried out for each system. The last 100 ns of each simulation were used for the analysis.

2.7. Statistical analysis

The two-tailed *t*-test method was employed to analyze the statistical significance of all the data in this study.

3. Results

3.1. Altering the phospholipid head distribution increases tolerance to octanoic acid

Phospholipids are the primary structural constituent of the cell membrane. A phospholipid molecule generally consists of a hydrophilic phosphate head and two hydrophobic fatty acid tails. In *E. coli*, there are three different phospholipids: PE, PG, and CL (Fig. 1) (Oliver et al., 2014). Head group diversity of the three phospholipids can be seen in Fig. 1. For PE, PG and CL, the specific head group is -CH₂-CH₂-NH₃⁺, -CH₂-CHOH-CH₂-OH and -CH₂-CHOH-CH₂-O-PG, respectively. The size, polarity and charge of these head groups are distinct. PE is neutral and typically accounts for nearly 70–90% of total phospholipids. PG is acidic and the second most abundant (10–25%), CL is also acidic, is the least abundant (< 5%) and exists in the septal/polar regions (Oliver et al., 2014). Fig. 1 shows the biosynthesis pathways for these phospholipids in *E. coli*. CDP-diacylglycerol (CDPG) is the common precursor, and the majority of the CDPG is used by phosphatidylserine synthase (PssA) to produce PE. Phosphatidylglycerophosphate synthase (PgsA) draws CDPG into the PG biosynthesis branch and two molecules of PG can subsequently be used by cardiolipin synthase (ClsA) to produce one molecule of CL. Therefore, PssA, PgsA and ClsA are key enzymes in phospholipid synthesis and altering their abundance is expected to change the relative abundance of these three head groups. To this end, genetic deletion of *pssA*, *pgsA* and *clsA* genes was attempted. The *clsA* gene was successfully deleted, but consistent with previous reports (Baba et al., 2006), *pssA* and *pgsA* were found to be essential in our condition. The Δ *clsA* strain was confirmed to lack detectable CL (Table 1) and, consistent with previous reports (Rowlett et al., 2017),

the CL-deficient strain had a decreased ($P = 0.04$) growth rate in defined media (Fig. 1).

Expression of *pssA*, *pgsA* and *clsA* was increased individually by chromosomal insertion of a second copy of each gene, regulated by the strong constitutive promoter M1-93 (Zhu et al., 2014; Tan et al., 2013), to obtain strains +*pssA*, +*pgsA* and +*clsA*. As expected, the relative abundance of PE, PG and CL significantly increased when each of these genes was overexpressed. Specifically, PE increased by 7% (from 88 ± 2 to 93.7 ± 0.4 mol%), PG increased by 38% (from $8.8 \pm 0.4\%$ to $12.1 \pm 0.3\%$) and CL increased by 12% (from $3.3 \pm 0.1\%$ to $3.7 \pm 0.2\%$) in the respective +*pssA*, +*pgsA* and +*clsA* strains relative to the control (Table 1).

The tolerance of these engineered strains to octanoic acid (C8), a representative membrane-damaging inhibitor, was assessed. Increasing the expression of *clsA* (+*clsA*) did not result in a significant increase in specific growth rate during challenge with C8 (Fig. 1). An increase in PG content (+*pgsA*) was found to compromise C8 tolerance: in the presence of 20 mM C8, the specific growth rate of +*pgsA* (0.17 h^{-1}) declined by 50% relative to the control strain (0.34 h^{-1} , $P < 0.01$) (Fig. S1). In contrast, an increase in PE content (+*pssA*) was found to significantly enhance tolerance to C8. In the presence of 20 mM C8, the specific growth rate of +*pssA* (0.44 h^{-1}) increased by 29% over the control strain (0.34 h^{-1} , $P < 0.01$) (Fig. S1). Since increasing phospholipid PE content resulted in the largest increase in C8 tolerance, we chose the corresponding strain, +*pssA*, for further analysis.

3.2. Increased PE abundance is associated with altered membrane properties

Membrane leakage is considered a primary mechanism of membrane damage and efforts to improve membrane integrity have been effective in increasing tolerance of membrane-damaging compounds (Lennen and Pfeleger, 2013; Royce et al., 2015; Jin et al., 2017). Cells with a compromised membrane can be penetrated by the SYTOX Green nucleic acid stain, as identified by flow cytometry (Roth et al., 1997). Herein, we observed that an increase in PE content was associated with a significant increase in membrane integrity. Specifically, the percentage of cells with intact membranes during challenge with 10 mM C8 was $89.0 \pm 0.3\%$, which is a 78% increase ($P < 0.001$) relative to the control strain ($50 \pm 1\%$) (Fig. 2A; Table S2). This increased membrane integrity is expected to decrease ion leakage (e.g. Na⁺, K⁺ and Cl⁻) and strengthen the associated transmembrane concentration gradients (Fig. 2F). Another important membrane property associated with carboxylic acid toxicity (Royce et al., 2013; Tan et al., 2016), membrane fluidity, was not changed in the +*pssA* strain (Table S2).

Membrane surface potential plays a critical role in cellular physiological activities, such as transport (Cerbon and Luna, 1991). Since PE is zwitterionic and its net charge is zero, an increase in PE content and decrease in PG and CL, both of which are acidic, is expected to decrease membrane surface negative potential. Consistent with our hypothesis, membrane surface negative potential decreased by 25% ($P < 0.05$) in the +*pssA* strain relative to the control during challenge with 10 mM C8 (Fig. 2B; Table S2). Membrane electrochemical potential ($\Delta\psi$) also impacts cellular physiological activities, such as cell division and energy metabolism (Kakinuma, 1998; Strahl and Hamoen, 2010). The control strain had a relatively low membrane potential of 0.70 ± 0.02 (DiOC₂(3) red/green fluorescence ratio) during challenge with 10 mM C8. In contrast, the membrane potential of the +*pssA* strain was increased by 120% to 1.53 ± 0.08 ($P = 0.001$) under same condition (Fig. 2C; Table S2).

The composition of the membrane can impact cellular surface chemistry, which might influence the interaction with extracellular inhibitors. The engineered +*pssA* strain showed a 46% increase in cellular hydrophilicity, and therefore decreased hydrophobicity, relative to the control when treated with 10 mM C8 (Fig. 2D; Table S2). This change is consistent with prior observations that lower surface

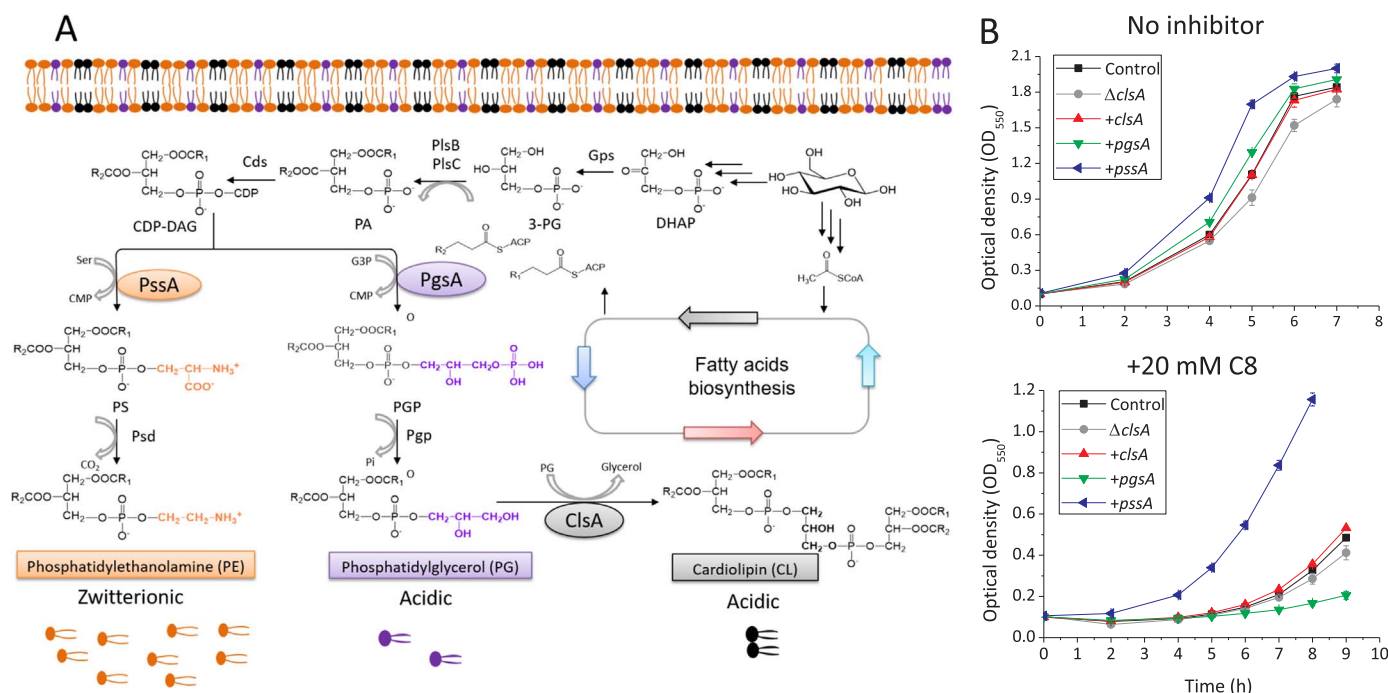


Fig. 1. Altering phospholipid head distribution impacts octanoic acid tolerance. (A) Phospholipid biosynthesis pathways in *E. coli*. G6P, glucose-6-phosphate; FBP, Fructose-1,6-bisphosphate; DHAP, dihydroxyacetone phosphate; 3-PG, glycerol-3-phosphate; PA, phosphatidic acid; CDP-DAG, cytidine diphosphate diacylglycerol; PS, phosphatidylserine; PE, phosphatidylethanolamine; PGP, phosphatidylglycerophosphate; PG, phosphatidylglycerol; CL, cardiolipin; Gps, glycerol-3-phosphate dehydrogenase; PlsB, glycerol-3-phosphate acyltransferase; PlsC, 1-acylglycerol-3-phosphate O-acyltransferase; Cds, CDP-diglyceride synthetase; PssA, phosphatidylserine synthase; Psd, phosphatidylserine decarboxylase; PgsA, phosphatidylglycerophosphate synthase; Pgp, phosphatidylglycerophosphatase; ClsA, cardiolipin synthase. The three enzymes selected here for expression tuning, PssA, PgsA and ClsA, are highlighted. (B) Engineering the abundance of the genes encoding phospholipid biosynthesis enzymes can significantly impact octanoic acid (C8) tolerance. Growth during challenge with 0 mM (upper) and 10 mM C8 (lower) in MOPS + 2% dextrose shake flasks at 220 rpm 37 °C with an initial pH of 7.0. Values are the average of at least three biological replicates with error bars indicating one standard deviation. $\Delta clsA$ means disruption of *clsA* gene in MG1655. For +*clsA*, +*pgsA* or +*pssA*, a second copy of each gene was inserted individually into the chromosomal DNA of *E. coli* MG1655 at the *ldhA* site and regulated by strong promoter M1-93. The *ldhA* gene was also deleted from MG1655 to serve as the Control strain.

Table 1

Distribution (wt%) of phospholipid head groups in engineered strains. All strains are derivatives of MG1655 and were cultured in MOPS + 2% dextrose with 10 mM C8 in shake flasks at 220 rpm 30 °C with an initial pH of 7.0. Values are the average of at least three biological replicates with the associated standard deviation. ND, not detected.

Strain	PG	CL	PE
$\Delta clsA$	12.8 ± 0.4	ND	87.2 ± 0.4
Control	8.8 ± 0.4	3.3 ± 0.1	87.8 ± 2.4
+ <i>clsA</i>	8.6 ± 0.3	3.7 ± 0.2	87.7 ± 1.3
+ <i>pgsA</i>	12.1 ± 0.3	3.2 ± 0.1	84.7 ± 2.1
+ <i>pssA</i>	3.7 ± 0.2	2.6 ± 0.3	93.7 ± 0.4

Values in bold indicate a significant ($P < 0.05$) difference from the Control strain.

hydrophobicity confers *E. coli* with improved tolerance to organic solvents (Aono and Kobayashi, 1997). This increased hydrophilicity of +*pssA* might be due to PE possessing a more polar head group relative to PG and CL (Fig. 1). We deemed that all these global membrane characteristics changes contribute to the robustness of +*pssA* strain when treated with representative membrane-damaging C8 (Fig. 1; Fig. 2F).

Organic acids, such as C8, can enter through the membrane and then dissociate in the cytoplasm, with the accumulating protons decreasing the intracellular pH even when the media pH is maintained at 7.0 (Royce et al., 2014; Jarboe et al., 2013). Therefore, the degree of intracellular acidification can serve as the indicator for C8 entry into cells. To this end, we measured the intracellular pH of both the control and +*pssA* strains and found that the intracellular pH of the +*pssA* strain was 6.68 during challenge with 10 mM C8, which observably increased relative to 6.28 in the control strain ($P < 0.03$) (Fig. 2E; Table S2). These results further confirmed the +*pssA* strain did block the entry of exogenous C8 into cell due to the robust membrane (Fig. 2F).

While our engineering efforts here targeted the distribution of the phosphate head groups, the distribution of most of the fatty acid tails was also found to be significantly altered in the +*pssA* strain, resulting in a significant increase in average tail length and relative abundance of unsaturated fatty acids, and decreased abundance of cyclic rings (Table 2). The association of increased average tail length and increased fatty acids tolerance has been previously reported for engineered (Sherkhanov et al., 2014) and evolved (Royce et al., 2015) strains. The relative abundance of the C16:1 and C18:1 unsaturated fatty acid tails increased from 32 ± 1% in the control strain to 44 ± 1% in the +*pssA* strain ($P = 0.007$). This change differs from previous reports where the fatty acids and ethanol tolerance was increased by decreasing the relative abundance of unsaturated fatty acids (Lennen and Pfleger, 2013; Luo et al., 2009), which highlights the fact that this membrane engineering strategy is distinct from those previously described.

3.3. Increasing *pssA* expression increased fatty acids production

While we observed that increased PE content was associated with enhanced tolerance of *E. coli* to C8, previous studies have shown that membrane components that are helpful in low amounts can sometimes be detrimental in higher amounts (Tan et al., 2016). To this end, different promoters with varied strengths (Tan et al., 2016, 2013; Lu et al., 2012) were employed to regulate the expression level of the second copy of *pssA* in order to further explore the relationship between PE abundance and C8 tolerance. We observed a dose-dependent relationship between PE content and tolerance to 10 mM C8 in the range we achieved. However, it is possible that at sufficiently high levels, the effect of increasing PE content may saturate, or even have a negative impact on tolerance. The construct with the M1-93 promoter was identified as the most C8-tolerant strain (Fig. 3A). This is not surprising,

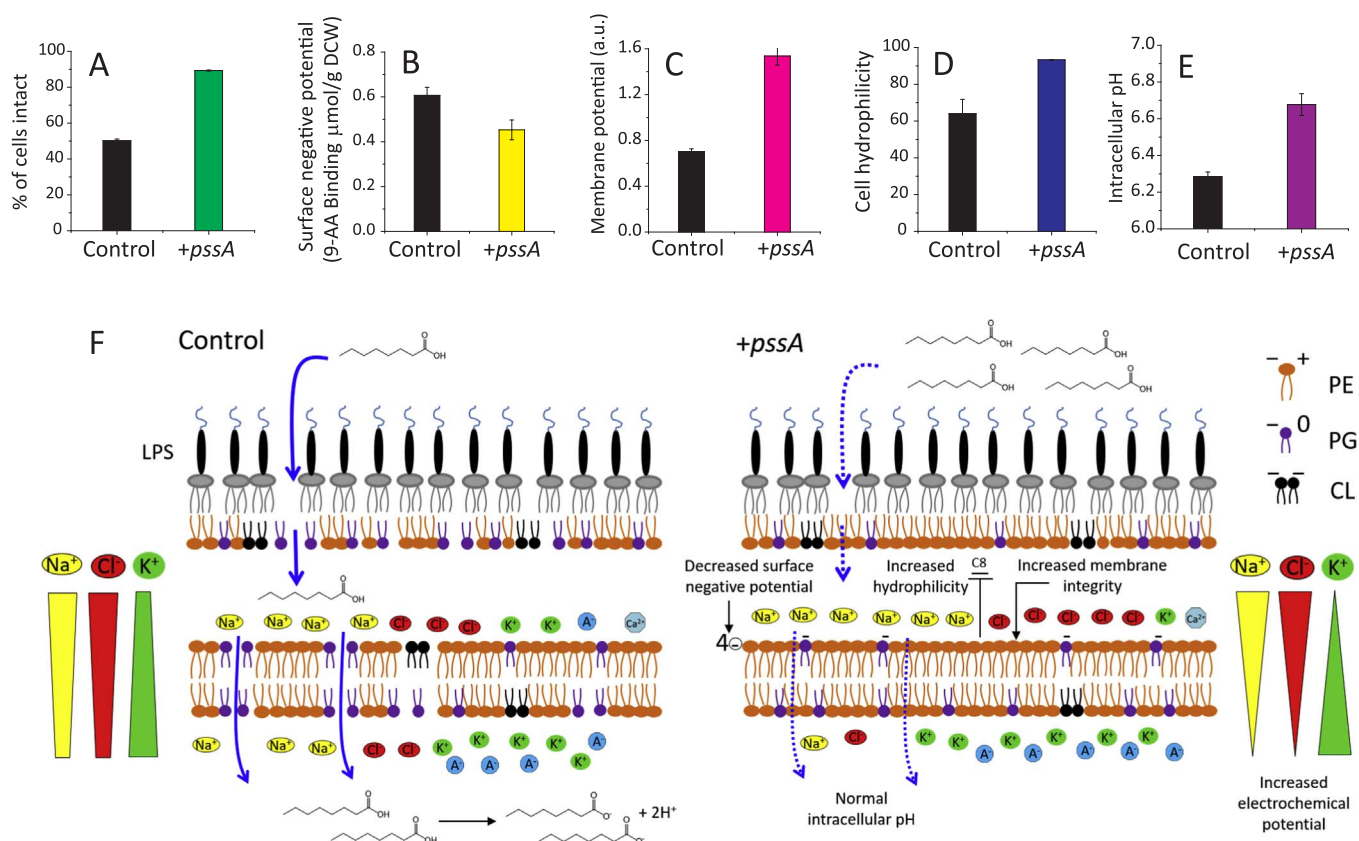


Fig. 2. +pssA significantly improves membrane integrity, membrane electrochemical potential, cellular hydrophilicity and intracellular pH during challenge with C8. (A) +pssA strain has a 78% increase in membrane integrity relative to the Control strain, as assessed by SYTOX permeability (B) Membrane surface negative potential decreased by 25% ($P = 0.01$) in +pssA. Membrane surface negative potential was assessed using monovalent cationic 9-aminoacridine (9-AA) fluorescence dye binding. (C) Membrane electrochemical potential increased by 120% in +pssA ($P < 0.01$) due to decreased leakage of ions (e.g. Na^+ , K^+ , and Cl^-). Membrane electrochemical potential was assessed by DiOC₂(3) red/green ratio. (D) Cell hydrophilicity increased by 46% for the +pssA strain relative to the control ($P = 0.001$), which means hydrophobicity decreased in +pssA strain. Hydrophobicity was assessed by measuring the microbial adhesion to hydrocarbons (MATH). (E) Intracellular pH increased in the +pssA strain ($P = 0.001$), presumably due to prevention of C8 entry and dissociation. (F) Summary of the membrane characteristics that were altered between the Control and +pssA strain. Penetration of membrane-damaging C8 solvent into the membrane hydrophobic core was alleviated by strengthened membrane in +pssA strain. These characteristics were all assessed after growth in the presence of 10 mM C8 in MOPS + 2% dextrose shake flasks at 220 rpm at 30 °C, initial pH 7.0. Values are the average of three biological replicates with error bars indicating one standard deviation. OM, outer membrane; PS, periplasmic space; IM, inner membrane. +pssA means a second copy of the pssA gene was inserted into the chromosomal DNA of *E. coli* MG1655 at *ldhA* site and regulated by strong promoter M1-93. The *ldhA* gene was also deleted from MG1655 to serve as the Control strain. C8, octanoic acid.

Table 2

Phospholipid fatty acid tail composition (mol%) of the control and +pssA strains assessed in MOPS + 2% dextrose with 10 mM C8, initial pH of 7.0, in shake flasks at 220 rpm and 30 °C. The Top6-midlog model (Khakbaz and Klauda, 2015) is shown for comparison. Values in bold font differ significantly ($P < 0.05$) in the experimental characterization of the two strains.

	Control		+PssA		Top6-midlog Model
	Experiment	Model	Experiment	Model	
C14:0	0.9 ± 0.2	0	0.584 ± 0.009	0	0
C16:0	46.1 ± 0.7	50	40 ± 1	41	44
C16:1	10.9 ± 0.3	10	7.22 ± 0.06	7.5	29
C16-CH ₃	0.96 ± 0.02	0	1.95 ± 0.06	0	0
C17cyc	15.0 ± 0.1	15	7.4 ± 0.1	7.5	9
C18:0	2.3 ± 0.1	5	3.2 ± 0.2	4	0
C18:1	21 ± 1	20	36.6 ± 0.9	40	15
C18-OH	0.48 ± 0.01	0	0.19 ± 0.01	0	0
C19cyc	2.5 ± 0.2	0	2.9 ± 0.3	0	0
Average length ^a	16.50 ± 0.03	16.5	16.85 ± 0.02	16.88	16.46
% unsaturation ^b	32 ± 1	30	44 ± 1	47.5	44
% cyclic ring ^c	17.5 ± 0.3	15	10.3 ± 0.4	7.5	9
PE/PG	10.0 ± 0.1	10.4	25.3 ± 0.3	25.7	4.2

^a $[14*(\text{C14:0}) + 16*(\text{C16:0} + \text{C16:1} + \text{C16-CH}_3 + \text{C17cyc}) + 18*(\text{C18:0} + \text{C18:1} + \text{C18-OH} + \text{C19cyc})]/100$.

^b C16:1 + C18:1.

^c C17cyc + C19cyc.

given that the M1-93 promoter exhibits generally strong activity (Zhu et al., 2014; Lu et al., 2012). The relationship between PE content and the associated promoter is consistent with previous *lacZ*-based characterization of promoter strength, except for M1-46, which has lower activity here than in previous work (Lu et al., 2012).

Having demonstrated that increased PE content is associated with increased tolerance to C8, we then tested the impact of this engineering strategy on C8 production. To this end, a control *E. coli* strain was constructed for C8 production. The AcrAB-TolC transporter complex has been found to contribute to free fatty acids efflux (Lennen et al., 2013) and thus these genes were overexpressed via chromosomal insertion. The +pssA manipulation was implemented in this strain, resulting in PssA-AcrAB-TolC strain. The pJMYEEI82564 plasmid (Royce et al., 2015) harboring thioesterase (TE) from *Anaerococcus tetradus*, which primarily hydrolyzes C8-ACP to release C8, was also used, resulting in strain +pssA-*acrAB-tolC-TE10*. Analogous manipulations were also performed to the control strain, Control-*acrAB-tolC-TE10*. When characterized in MOPS + 2% (wt/v) glucose minimal salts medium, the +pssA-*acrAB-tolC-TE10* strain produced 220 ± 4 mg/L of C8 and 280 ± 6 mg/L of total fatty acids (TFA), which was 46% and 40% higher than the corresponding control strain (150 ± 10 mg/L of C8, 200 ± 13 mg/L of TFA) respectively (Fig. 3B). These results demonstrate that the membrane engineering strategy of increasing the relative abundance of the PE phospholipid head is effective in increasing not just C8 toxicity, but also C8 production.

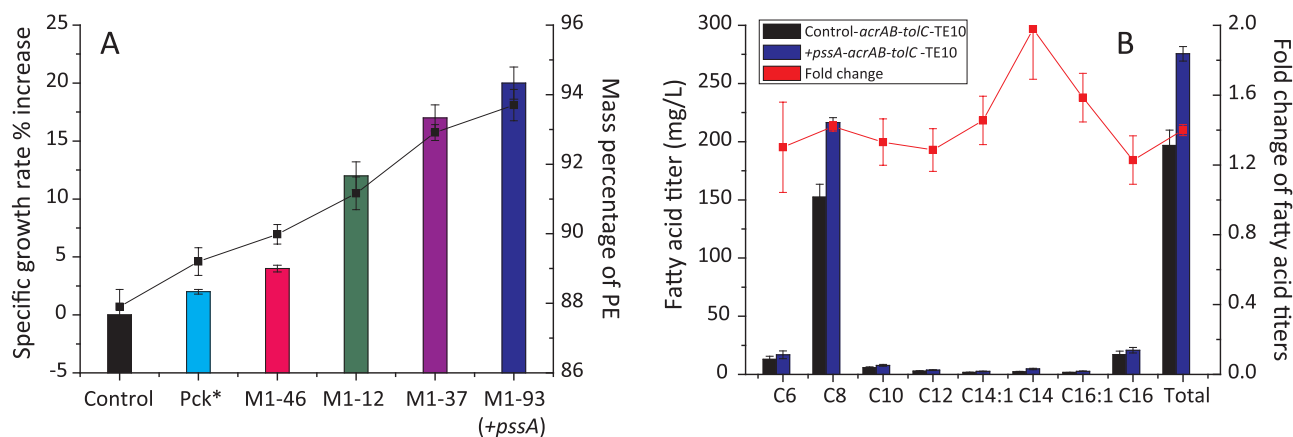


Fig. 3. Increasing the relative abundance of the PE phospholipid head group increases both tolerance and production of C8. (A) Relationship between PE content and C8 tolerance. Column, specific growth rate % increase. Solid line, relative abundance of PE in the membrane. For modulating expression of *pssA*, a gene copy was inserted into the chromosomal DNA of *E. coli* MG1655 at *ldhA* site and regulated by promoters Pck*, M1-46, M1-12, M1-37 and M1-93. The strain M1-93-*pssA* is also referred to as the +*pssA* engineered strain. The *ldhA* gene was deleted from MG1655 to generate the Control strain. Specific growth rate changes were analyzed during challenge with 10 mM C8 in MOPS + 2% dextrose shake flasks at 220 rpm 30 °C with an initial pH of 7.0. (B) Production of fatty acids in MOPS + 2% dextrose mineral salts medium at 30 °C, initial pH 7.0 over 72 h. Both strains harbor the pJMYEEI82564 plasmid, which encodes thioesterase TE10 from *Anaerococcus tetradius*. Values are the average of three biological replicates with error bars indicating one standard deviation. Control-*acrAB-tolC-TE10*: *AcrAB-TolC* + pJMYEEI82564; +*pssA-acrAB-tolC-TE10*: +*pssA-AcrAB-TolC* + pJMYEEI82564.

3.4. Membrane engineering increases simulated membrane thickness and decreases chemical penetration

The experimental analyses described above show that increasing the relative abundance of the PE phospholipid head group significantly alters a variety of membrane and cell surface properties. Molecular dynamics simulations were used to further our understanding of this membrane engineering strategy. Two membrane models were initially used: one representing the control strain and one representing the +*pssA* engineered strain. The relative abundance of the head groups and fatty acid tails in these models (Tables S3 and S4) were based on experimental data (Tables 1, 2). CL was not included in our membrane models, because these lipids are known to segregate to the polar and septal regions to induce curvature (Nishibori et al., 2005) and our approach is to focus on membrane structure outside these minor regions in the bacteria. Snapshots of the end of the simulations are shown in Fig. 4A.

In the absence of inhibitors, the control and +*pssA* membrane models both had a predicted surface area of 59 Å²/lipid (Table 3). The electron density profiles (EDPs) had a similar shape for both models (Fig. 4C), but a slight shift toward the center of membrane was seen at the peak point of total electron density profile of the control model. The simulated EDPs and volume probability profiles of the lipids and water were used to calculate the head-to-head group thickness (D_{HH}), bilayer thickness (D_B), and hydrophobic core thickness ($2D_C$) (Table 3). For each of these metrics, the +*pssA* membrane model has a higher value than the control model. Among these thicknesses, D_{HH} was statistically larger in the +*pssA* model ($P = 0.03$). While our experimental observation of an increase in the average fatty acid tail length in the +*pssA* strain (Table 2) suggests an increase in membrane thickness, these simulation results provide a more direct measure of membrane thickness and represent the diffusion barrier across the membrane.

To compare the fluidity of the two membrane models in the absence of inhibitors, the order parameters of fatty acid chains (S_{CD}) were calculated as the average of C4 to C6 of *sn*-1 for all lipids (Table S5). These were the same when comparing the two models in the absence of any inhibitors, which is in agreement with the equivalent lipid average surface areas described above. The area compressibility modulus (K_A) is the measure of rigidity of the membrane and also was not statistically different between the two models ($P = 0.16$). The fluidity experimentally measured by membrane polarization (Table S2) is similar between the strains, which might suggest that this is in agreement with our K_A findings. However, membrane polarization is more a measure of

lipid diffusion whereas K_A is an elastic measure of force required to laterally stretch the membrane. Thus, while the membrane thickness metrics suggest that the +*pssA* strain has a thicker membrane than the control, the lateral rigidity of these two membranes is predicted to be similar.

In addition to analyzing the control and +*pssA* membrane in the unperturbed condition, we also simulated these membranes during challenge with approximately 4.6 mol% ethanol. Ethanol was selected as a representative membrane-damaging compound due to it being a simple alcohol and because the +*pssA* engineered strain showed an approximately 10% increase in specific growth rate during challenge with 2% (v/v) (approximately 0.6 mol%) ethanol (Fig. 5). Ethanol penetration into the bilayers of both membrane types is evident in the snapshots in Fig. 4B. Consequently, the surface area per lipid increased in the presence of ethanol from approximately 59 to 67 Å²/lipid for both models (Table 3). Also, for both models, the total electron density profile peaks were shifted towards the center of the bilayer in the presence of ethanol (Fig. 4C; Fig. S3). For the model of the wild-type membrane, all measures of membrane thickness were substantially and significantly decreased in the presence of ethanol (Table 3). Similar decreases were observed in the +*pssA* model for D_{HH} and D_B . However, the impact of ethanol on the hydrophobic core thickness was substantially dampened relative to the wild-type strain (Table 3; Fig. S2). Specifically, the hydrophobic core thickness of the control membrane decreased by 1.4 Å ($P = 0.03$) during ethanol challenge, but only a 0.14 Å ($P = 0.6$) decrease was observed for the +*pssA* model. These results indicate that during exposure to ethanol, the +*pssA* membrane has a thicker bilayer and hydrophobic core than the control membrane and that its hydrophobic core thickness is more resistant to perturbation by ethanol.

For both models, the upper chain order parameter S_{CD} decreased as the ethanol concentration increased (Table S5), which is consistent with the decreased membrane thickness and increased surface area per lipid. However, the +*pssA* model had a significantly higher S_{CD} value for the DOPE phospholipid during challenge with ethanol relative to the control model ($P < 0.001$), which may contribute to the increase in hydrophobic core thickness. The penetration of ethanol into these two membrane types was quantified with component electron density profiles (Fig. S4). For the +*pssA* membrane, the electron density peaks for both the phosphate and carbonyl groups decreased as the ethanol concentration increased, due to increases in the surface area per lipid and penetration of ethanol into the head group region. In the presence of 4.6 mol% ethanol, the ethanol penetration into the bilayer is clearly

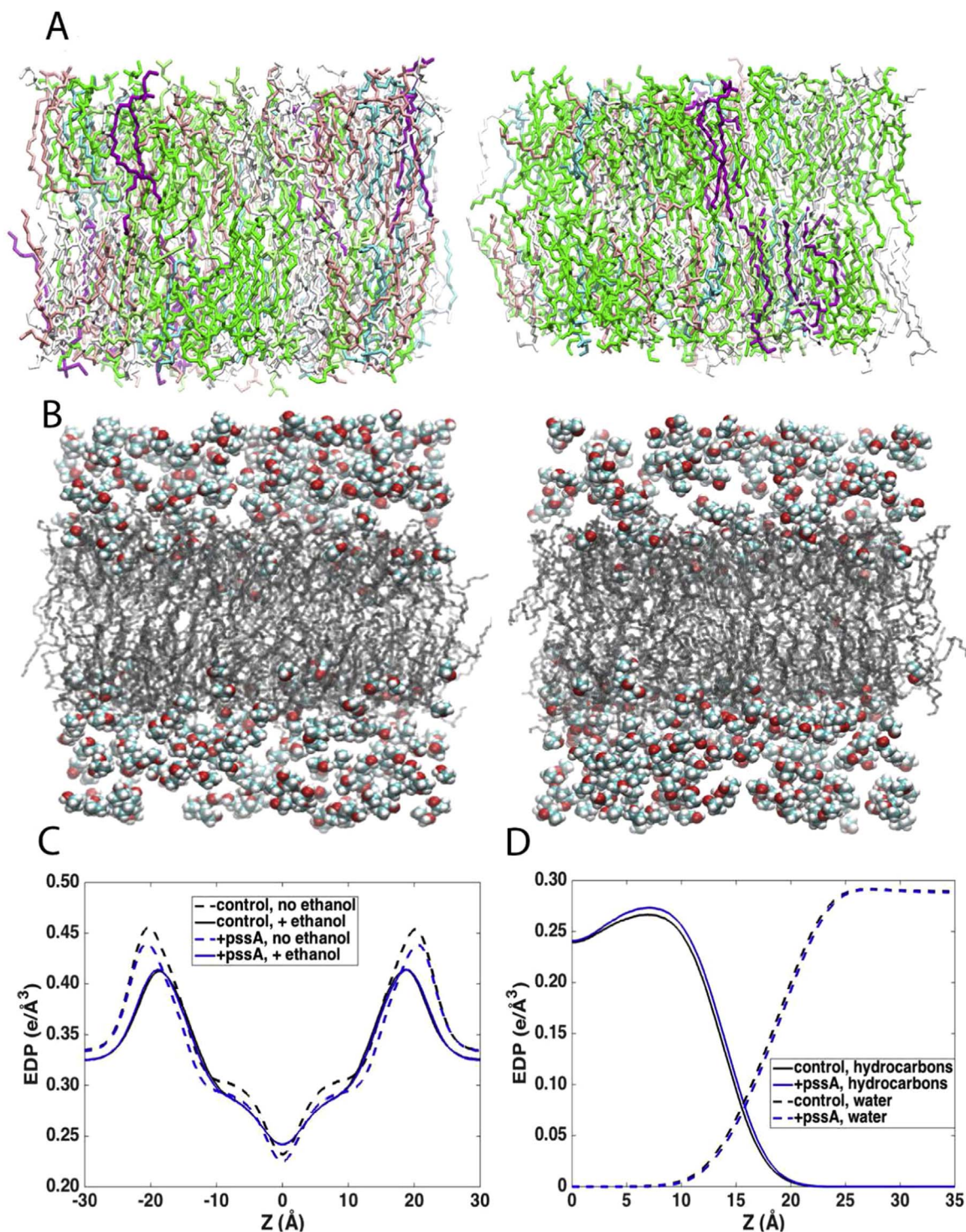


Fig. 4. Molecular dynamics simulation of the control and +pssA membranes with and without ethanol. (A) Left: Snapshot of simulation for the control membrane model. DOPE is shown in light green, DPPE in grey, DSPE in violet, DYPE in cyan, PMPE in pink, and PMPG in dark green. Right: Last snapshot of simulation for membrane in +pssA model. Same color code was used. (B) Left: Simulation snapshot of the control membrane model with 4.64 mol% ethanol. Right: Simulation snapshot of the +pssA membrane model with 4.56 mol% ethanol. Lipids are shown in grey. Hydrogen atoms are not shown for clarity. Ethanol molecules are shown in van der Waals spheres. (C) Total electron density profiles of +pssA and control models with 0 and 4.6 mol% ethanol. (D) Component electron density profiles of water and hydrocarbons ($\text{CH}_3 + \text{CH}_2 + \text{CH}$) in +pssA and control models with 4.6 mol% ethanol.

reduced (Fig. S4C) for the +pssA model compared to control.

Overall, structural changes in the +pssA membrane led to increased ethanol resistance. The stress tolerant strain ultimately results in a thicker bilayer for the hydrophobic core and reduced ethanol penetration. Ultimately, this may decrease permeation of representative membrane-damaging compounds, which is consistent with our experimental C8 results (Figs. 1, 2).

3.5. Changes in both the head group and fatty acid chain distribution impacts simulated membrane thickness

As described above, experimental characterization showed not only an altered distribution of the phospholipid head groups in the +pssA strain, but also an altered distribution of the fatty acid tails (Table 2). In order to distinguish the impact of the head group change from the

Table 3

Predicted properties of the model membranes. The Top6-mid log model is shown for comparison (Khakbaz and Klauda, 2015). KA is the area compressibility modulus, DHH is the head-to-head group thickness, DB is the bilayer thickness, and 2DC is the hydrophobic core thickness. For the hybrid models, X/Y indicates head group model composition (X) and fatty acid chain model composition (Y). Values are the average of three simulations with the accompanying standard deviation. Additional data for the +*pssA* model during ethanol challenge is given in Table S4.

Model	Ethanol (mol%)	Surface Area (Å ² /lipid)	K _A (N/m)	D _{HH} (Å)	D _B (Å)	2D _C (Å)
Top6-midlog	0	61.26 ± 0.04	0.29 ± 0.01	38.0 ± 0.1	38.15 ± 0.03	30.36 ± 0.03
Control	0	59.0 ± 0.2	0.175 ± 0.002	40.6 ± 0.1	38.67 ± 0.07	31.8 ± 0.1
+ <i>pssA</i>	4.64	66.9 ± 0.2 ⁺	0.076 ± 0.001 ⁺	37.3 ± 0.2 ⁺	34.9 ± 0.1 ^{+,+}	30.4 ± 0.7 ^{+,+}
	0	59.0 ± 0.2	0.16 ± 0.01	41.0 ± 0.0	39.0 ± 0.1	32.0 ± 0.1
+ <i>pssA</i> /control	4.56	66.8 ± 0.1 ⁺	0.079 ± 0.005 ⁺	37.5 ± 0.2 ⁺	35.6 ± 0.2 ⁺	31.9 ± 0.4
+ <i>pssA</i> /control	4.67	65.9 ± 0.3 ⁺	0.096 ± 0.002 ⁺	37.9 ± 0.2	35.4 ± 0.1	30.95 ± 0.03 ⁺
control/+ <i>pssA</i>	4.50	67.8 ± 0.4 ⁺	0.086 ± 0.003	37.5 ± 0.2	35.1 ± 0.2	31.46 ± 0.5

Bold font indicates a significant difference from the control model, assessed only in the presence of ethanol.

* indicates a significant difference (P < 0.05) in the presence of ethanol relative to the no-ethanol condition for the same model, assessed only for the control and +*pssA* models.

⁺ indicates a significant difference from the +*pssA* model, assessed only in the presence of ethanol.

impact of the fatty acid tail change, we built two hybrid membrane models (Table S3). The +*pssA*/control (head group/tail) hybrid model has the same head group composition as the +*pssA* model, while maintaining the fatty acid chains composition of control model. The second control/+*pssA* hybrid model has the same head group composition as the control strain and the fatty acid chains from the +*pssA* model. Both of these hybrid models were assessed at ethanol concentrations of roughly 4.6 mol%.

A significant increase in head-to-head and bilayer thickness was predicted for the hybrid +*pssA*/control model relative to the control (Table 3). Contrastingly, the control/+*pssA* model did not show a significant difference in D_{HH} or D_B relative to the control. Therefore, the increase in bilayer thickness D_B observed for the +*pssA* model during ethanol challenge can be attributed to the change in the head group distribution.

However, it appears that the increase in hydrophobic core thickness in the +*pssA* strain relative to the control cannot be attributed only to the change in head group distribution or the change in fatty acid tail distribution. A significant increase in D_C was observed only in the +*pssA* model, not in either of the hybrid models (Table 3). This is likely the result of coupling of properties between the tail and lipid head

group. For +*pssA*/control, having an increase in the PE content results in a decrease in the surface area per lipid due to head group hydrogen bonding. However, for control/+*pssA* the area increases relative to the control due to the bulkier acyl chains. When these head group and tails are combined in a membrane with no change in surface area per lipid from the control (Table 3). The K_A appears to be more complicated, as both hybrid models show an increase in values compared to the control, possibly due to more hydrogen bond character in the +*pssA*/control model and chain tangling in control/+*pssA*.

Overall, we can conclude that the changes in the distribution of both the head groups and fatty acid tails contribute to a thicker membrane. Specifically, the change in the head group distribution influences the bilayer thickness while the change in both the head group distribution and the acyl chains influences the hydrophobic core thickness. These changes in the +*pssA* strain act together, but independently, to increase the distance for permeation across the membrane.

3.6. Increased *pssA* expression enhanced tolerance to other bio-products, inhibitors and adverse conditions

In this study, C8 was used as a representative membrane-damaging

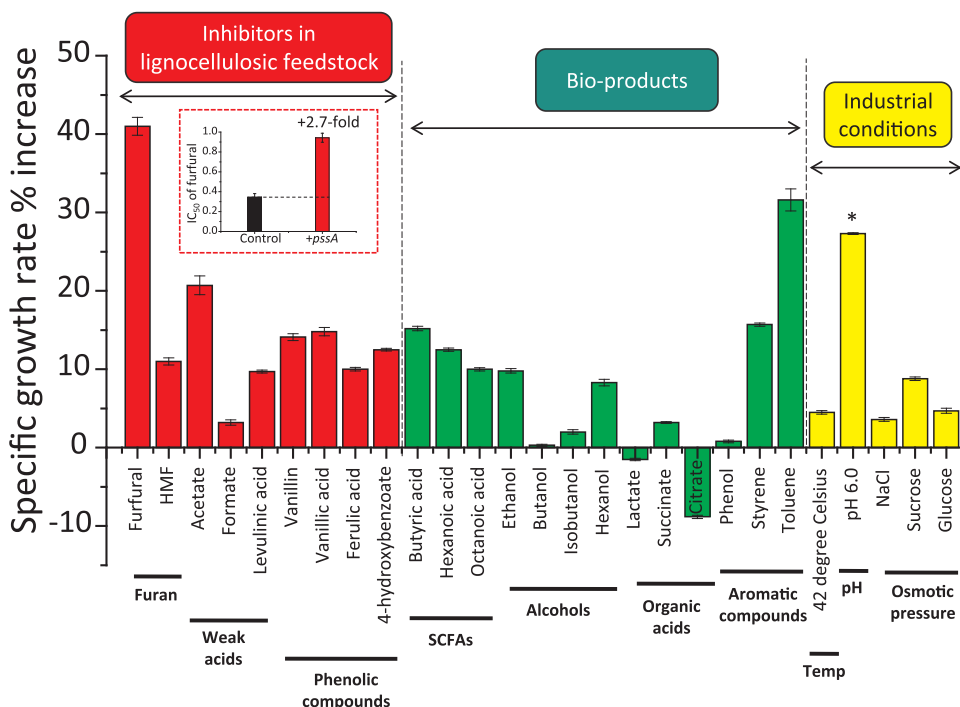


Fig. 5. Increasing the relative abundance of the PE head group increases tolerance to other inhibitory compounds and environmental stressors. Specific growth rate changes compare the engineered +*pssA* strain to the Control strain. +*pssA* means a second copy of *pssA* gene was inserted into the chromosomal DNA of *E. coli* MG1655 at *ldhA* site and regulated by strong promoter M1-93. The *ldhA* gene was deleted from MG1655 to generate the Control strain. The inset shows the increase in the 50% inhibitory concentration (IC₅₀) of furfural relative to the control. Values are the average of at least three biological replicates with error bars indicating one standard deviation. Asterisk (*), cell mass increase. SCFA, short chain fatty acids. Temp, Temperature. All conditions except challenge with formate, butanol, and phenol have a P value < 0.05. The final concentrations of each chemical are given in Table S6.

compound. Given that an increase in PE content is a general membrane change, we hypothesized that it should not only confer *E. coli* with increased robustness to C8, but may also be effective in other conditions that possibly cause membrane damage. To this end, three general classes of inhibitory stresses were considered: (A) inhibitors found in hydrolysate of lignocellulose, (B) industrial fermentation products, and (C) adverse industrial conditions (Fig. 5). Each of the investigated bio-products is an attractive biorenewable chemical and each of the processing conditions can impact the process cost.

There are three main classes of inhibitors in dilute acid-treated lignocellulose feedstock: furans, weak carboxylic acids and phenolic monomers (Mills et al., 2009). Furans can cause DNA damage and inhibit metabolic processes (Mills et al., 2009; Miller et al., 2009). Weak carboxylic acids, such as acetate, can disrupt transmembrane potential and decrease intracellular pH (Mills et al., 2009; Trcek et al., 2015). Some phenolic monomers have been shown to cause membrane leakage and repress *E. coli* respiration (Mills et al., 2009; Fitzgerald et al., 2004). For cost-effective utilization of lignocellulosic biomass, construction of inhibitor-resistant host strains is desirable. We observed that increasing membrane PE content improved tolerance to most of these inhibitors (Fig. 5). Most dramatically, the +*pssA* strain had a 41% increase in its specific growth rate (0.36 h^{-1}) relative to the control strain (0.25 h^{-1}) in the presence of 1.0 g/L furfural ($P < 0.001$). Further analysis showed that the +*pssA* strain has a 2.7-fold increase in the concentration of furfural required for 50% inhibition (IC_{50}), from 0.34 g/L to 0.94 g/L (Fig. 5). Increased robustness was also observed to another furan derivative, hydroxymethylfurfural (HMF). In the presence of 2 g/L of HMF, the specific growth rate of +*pssA* was 12% higher ($P < 0.001$) than the control strain. For weak carboxylic acids, the +*pssA* strain had a 21% higher specific growth rate ($P < 0.001$) during challenge with 1.8 g/L of acetate, and it also had significantly increased tolerance to levulinic acid (Fig. 5). For phenolic monomers, the +*pssA* strain showed a roughly 10% increase in specific growth rate relative to the control strain when challenged with vanillin, vanillic acid, ferulic acid and 4-hydroxybenzoate ($P < 0.05$) (Fig. 5).

Considering that the +*pssA* strain showed improved tolerance to individual inhibitors known to be present in lignocellulose-derived feedstocks, and it also increased the production of bio-octanoic acid (Fig. 3B), we then tested them in combination. Three representative inhibitors, furfural, acetate and vanillic acid (FAV) were added to MOPS + 2% (wt/v) glucose minimal salts medium for bio-octanoic acid production at final concentrations of 0.8, 1.2 and 0.5 g/L, respectively. The engineered +PE strain, +*pssA*-*acrAB*-*tolC*-TE10, produced $155 \pm 5 \text{ mg/L}$ of C8 and $216 \pm 8 \text{ mg/L}$ of TFA, which is 66% and 42%

more than the Control-*acrAB*-*tolC*-TE10 ($93 \pm 11 \text{ mg/L}$, $153 \pm 14 \text{ mg/L}$), respectively (Fig. 6). This result confirms the usefulness of this engineering strategy during the production of a membrane-damaging bio-product in the presence of biomass-derived inhibitors. However, when we tested the effect of the +PE engineering strategy on the utilization of corn stover acid hydrolysate, a decrease in both C8 and TFA titers was observed relative to the control strain (Fig. S5). These results suggest that there may some inhibitor present in the hydrolysate whose toxicity was increased by this membrane engineering strategy.

Next, four different groups of bio-products were considered: short-chain fatty acids, organic alcohols, organic acids and other aromatic compounds distinct from those selected as representative of lignocellulose-derived feedstocks. Similar to the results observed for C8, increased PE abundance also increased tolerance to even shorter chain butyric acid (C4) by 15% and hexanoic acid (C6) by 13%, respectively. For alcohols, although increased PE abundance had a limited effect on tolerance to 0.6% (v/v) butanol or isobutanol, it did enable a 10% increase in specific growth rate during challenge with 2% (v/v) ethanol, which is consistent with our membrane modeling results described above, and also enabled a 7% increase ($P < 0.05$) in specific growth rate when challenged with 0.1% (v/v) hexanol. Each of these four alcohols has previously been shown to inhibit the growth of *E. coli*, but with distinct modes of toxicity (Brynildsen and Liao, 2009; Royce et al., 2015; Ingram and Vreeland, 1980). Additionally, the +*pssA* engineered strain had significantly increased tolerance to styrene (16%) and toluene (32%) ($P < 0.01$) relative to the control strain (Fig. 5).

In addition to specific inhibitory chemicals, the +PE membrane engineering strategy was also found to elevate robustness to some harsh conditions. When grown in medium with an initial pH of 6.0, the +*pssA* strain showed a 28% increase in final cell density OD_{550} , from 0.57 to 0.73 ($P < 0.001$). This increased acid resistance could reduce base requirements, and therefore reduce operating costs, and also decrease the vulnerability to contamination. The +*pssA* strain also increased specific growth rate by 9% in the presence of 240 mM sucrose and by 5% in the presence of 10% (wt/v) glucose ($P < 0.05$) (Fig. 5). Both of these compounds increase ionic osmotic pressures, which suggests that this membrane engineering strategy may be useful to conditions with high osmotic pressure and high-sugar fermentation. In conclusion, the +*pssA* engineering strategy conferred *E. coli* with improved robustness to a variety of inhibitory feedstocks, bio-products and conditions.

4. Discussion and conclusions

In the construction of microbial biocatalysts for production of

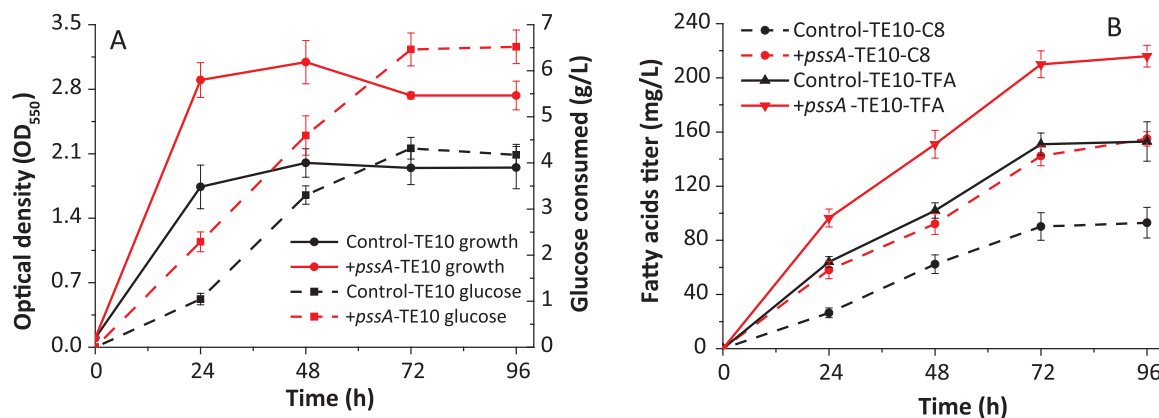


Fig. 6. Increasing the relative abundance of PE increased fatty acid production in the presence of model biomass-derived inhibitors. Production of octanoic acid (C8) and total fatty acids (TFA) was assessed in mineral salts medium (MOPS + 2% (w/v) dextrose) containing 0.8 g/L of furfural, 1.2 g/L of acetate and 0.5 g/L of vanillic acid at 30 °C, initial pH 7.0. Both strains carry the pJMYYEII82564 plasmid, which harbors thioesterase 10 (TE10) and have a second genomic copy of *acrAB* and *tolC* transporters under the control of promoter pM1-93. Values are the average of three biological replicates with error bars indicating one standard deviation. C8, octanoic acid, TFA, total fatty acids. Control-TE10: *acrAB*-*tolC*+pJMYYEII82564; +*pssA*-TE10: +*pssA*-*acrAB*-*tolC*+pJMYYEII82564.

biorenewable fuels and chemicals at economically viable titers and yields on a large scale, toxicity of the bio-product and/or the feedstock is often problematic and frequently attributed, at least in part, to membrane damage (Lennen et al., 2011; Liu et al., 2013; Royce et al., 2013; Zaldivar and Ingram, 1999; Huffer et al., 2011). Given the magnitude of this problem, modification of the membrane composition in order to increase its robustness is an attractive approach. Currently, most membrane engineering efforts have focused on changing the distribution of the phospholipid fatty acids tails, particularly in terms of fatty acid length and abundance and conformation of double bonds and cyclic groups (Lennen and Pfleger, 2013; Luo et al., 2009; Tan et al., 2016; Besada-Lombana et al., 2017; Sherkhanov et al., 2014).

Previous simulations of lipid membranes demonstrated the variability of the interaction of different phospholipid head groups with membrane-penetrating molecules, such as ethanol (Konas et al., 2015), suggesting that altering the distribution of these head groups could change the sensitivity of the membrane to such compounds. However, reports of experimental characterization of *E. coli* strains deficient in the PE, CL or PG/CL head groups concluded that such changes had a largely negative impact on cell physiology and the response to environmental stresses (Rowlett et al., 2017). Here, we report that increasing the expression of a gene specific to synthesis of the PE head group, without eliminating PG or CL production, increased tolerance of a variety of chemical inhibitors, such as short-chain fatty acids, furans, acetate, ethanol, and toluene (Figs. 1, 3 and 5), and industrially-relevant harsh conditions, such as high temperature, low pH, and high osmotic pressure (Fig. 5). Our strategy of increasing PE content also seems to be novel in the context of microbial response mechanisms (Weber and de Bont, 1996; Ramos et al., 2002). Specifically, in the presence of toluene, *Pseudomonas* strains decreased the relative abundance of PE while increasing PG and CL (Ramos et al., 2002), while here we observed that increasing PE content while decreasing PG and CL increased the specific growth rate in the presence of toluene by 30% relative to the corresponding control strain (Fig. 5).

Molecular dynamics simulations of the +*pssA* membrane showed an increased bilayer (D_B) and hydrophobic core thickness during ethanol challenge relative to the control membrane (Table 3). This increased resistance of the +*pssA* model membrane core to penetration by ethanol is consistent with the increased membrane integrity (Fig. 2A) and with the increased resistance of the +*pssA* strain to intracellular acidification by exogenous octanoic acid (Fig. 2E). The increase in abundance of the electron carrier lipid ubiquinone-8 (Q8) during osmotic stress has also been suggested as a strategy of increasing the membrane hydrophobic thickness (Sevin and Sauer, 2014), though the branched-chain Q8 could also possibly increase the membrane rigidity by increasing the lateral compressibility modulus (Lim and Klauda, 2011).

Given previous reports that altering the phospholipid head group distribution has little impact on the fatty acid tail distribution (Rowlett et al., 2017), it was surprising that nearly all fatty acid tails had a significantly altered relative abundance in the +*pssA* strain compared to the control strain (Table 2). The fact that the +*pssA* strain has substantial changes in both the phospholipid head groups and in the fatty acid tails makes it challenging to distinguish the contribution of these two molecule types to the physical properties of the engineered membrane. The molecular dynamics simulations played a vital role in assessing the relative effects of these changes by allowing the generation and assessment of two hybrid models which would have been very difficult to develop in an experimental system. Besides being useful in addressing solvent tolerance, this simulation strategy can probably also be applied to other membrane-damaging conditions, such as the role of Q8 in osmotic stress tolerance (Sevin and Sauer, 2014).

Many membrane physical characteristics were found to be altered in the +*pssA* engineered strain (Fig. 2). We observed a substantial increase in membrane integrity during octanoic acid challenge in the +*pssA* strain (Fig. 2A), similar to previous reports of an association

between membrane integrity and octanoic acid tolerance (Lennen and Pfleger, 2013). These prior efforts to increase membrane integrity have included an increase in the average length of the phospholipid tails (Sherkhanov et al., 2014), with an increase in average length also observed in the +*pssA* strain (Table 2), and decreasing the abundance of unsaturated lipid tails (Lennen and Pfleger, 2013), where the +*pssA* strain actually had an increase in unsaturated fatty acid abundance (Table 2). It is also possible that the change in head group distribution contributes to the altered membrane integrity. Specifically, the PE head group is zwitterionic, and thus increased PE abundance could result in fewer instances of charge repulsion by the negatively-charged PG and CL head groups (Fig. 2F). However, the models predict similar surface area per lipid values for both strains (Table 3). The increased membrane integrity could instead be attributed to the thicker hydrophobic core of the +*pssA* membrane and its increased resistance to chemical penetration, which is due to both the change in head group distribution and the change in lipid tail distribution.

Changes in the membrane surface negative potential and the membrane electrochemical potential were also observed (Fig. 2). Our observed association of increased membrane electrochemical potential with increased tolerance is consistent with the recent report that increasing the opposing potassium (K^+) and proton (H^+) electrochemical membrane gradients in *Saccharomyces cerevisiae* increased resistance to multiple alcohols (Lam et al., 2014). Moreover, the membrane-associated electron transport chain generates the proton motive force ($\Delta\mu$), which is usually directed inward, driving H^+ flux into the cytoplasm and ATP formation. The proton motive force is a function of the membrane electrochemical potential $\Delta\psi$ and the hydrogen ion chemical gradient (ΔpH) (Fischer et al., 2000) and thus it is possible that the engineered +*pssA* strain may have increased ATP production, though this was not measured. Note that previous characterization of strains lacking PE or CL showed decreased ATP content, but no change in membrane potential relative to the corresponding wild-type control (Rowlett et al., 2017).

The +*pssA* strain was found to have a substantial decrease in cell surface hydrophobicity (Fig. 2D), consistent with reports that tuning *S. cerevisiae* cell surface hydrophobicity can impact tolerance of biomass hydrolysate (Westman et al., 2014) and solvents, such as nonane (Perpina et al., 2015). This decrease in hydrophobicity for the +*pssA* strain can possibly be attributed to the fact that the PE head group ($-CH_2-CH_2-NH_3^+$) is more polar ($-CH_2-CHOH-CH_2-OH$) than the PG and CL groups ($-CH_2-CHOH-CH_2-O-PG$). *E. coli* strains lacking PE or CL have been reported to have altered ability to form biofilms and adhere to surfaces (Rowlett et al., 2017), though hydrophobicity of these strains was not reported. The octanol/water partition coefficient K_{OW} is widely recognized as being directly related to a molecule's toxicity (Inoue and Horikoshi, 1989) and similar to other membrane engineering efforts (Tan et al., 2016), we observed a dual relationship between the K_{OW} value for the organic acids tested here and the resulting increase in specific growth rate of the +*pssA* strain (Fig. S6). Specifically, the +*pssA* strategy was most helpful for increasing tolerance of organic acids with a log K_{OW} value between -0.5 and 1.0 .

Although product toxicity is often regarded as a primary limiter of strain performance, increased resistance does not always lead to increased production. Here, our rational membrane design of enabling PE increase not only improved tolerance to exogenously added C8 but also remarkably increased the C8 titer. The robust +*pssA* membrane was expected to block the re-entry of C8 from the broth and thus efficiently alleviate the toxicity. Increased C8 production was also observed even under lignocellulose-derived FAV inhibitors conditions. These examples not only demonstrate the effectiveness of the +*pssA* engineering strategy for increasing biocatalyst performance, but also suggest its potential for application to utilization of toxic lignocellulose feedstock for biorenewables production, which can achieve the goal of using cheap feedstocks with inhibitory components to produce bio-products at higher titers. Although previous studies of furan toxicity in *E. coli*

have not reported observation of membrane damage, (Mills et al., 2009; Zaldivar et al., 1999), we found that the +*pssA* strain had drastically improved tolerance to furfural.

Author contributions

L.R.J., Z.T. and J.B.K. designed research; Z.T., Y.C., J.L., and J.M.Y. performed experimental research, and P.K. performed theoretical research; Z.T., J.V.S., L.R.J., P.K. and J.B.K. analyzed data; and Z.T., P.K., L.R.J. and J.B.K. wrote the paper.

Acknowledgments

Funding for the Iowa State University authors was provided by the NSF Engineering Research Center for Biorenewable Chemicals (CBIRC), NSF Award number EEC-0813570. Funding for this project for the University of Maryland authors was provided from NSF (MCB-1149187 & CBET-1604576). The funders had no role in study design, data collection and analysis, decision to publish, or preparation of the manuscript. Computational resources utilized the High Performance Computing Clusters (HPCC) at the University of Maryland (Deepthought and Deepthought2) and Maryland Advanced Research Computing Center (MARCC) managed by Johns Hopkins University and the University of Maryland. We thank ISU Flow Cytometry Facility for help with SYTOX Green cells analysis, membrane potential analysis, and ISU W.M. Keck Metabolomics Research Laboratory for help with membrane polarization analysis and GC-MS analysis. We profusely thank Nancy Nichols and Sarah Frazer from National Center for Agricultural Utilization Research, U.S. Department of Agriculture for providing the corn stover hydrolysate and composition analysis.

Appendix A. Supporting information

Supplementary data associated with this article can be found in the online version at <http://dx.doi.org/10.1016/j.ymben.2017.08.006>.

References

- Aono, R., Kobayashi, H., 1997. Cell surface properties of organic solvent-tolerant mutants of *Escherichia coli* K-12. *Appl. Environ. Microbiol.* 63 (9), 3637–3642.
- Atsumi, S., Cann, A.F., Connor, M.R., Shen, C.R., Smith, K.M., Brynildsen, M.P., Chou, K.J., Hanai, T., Liao, J.C., 2008. Metabolic engineering of *Escherichia coli* for 1-butanol production. *Metab. Eng.* 10 (6), 305–311. <http://dx.doi.org/10.1016/j.ymben.2007.08.003>.
- Baba, T., Ara, T., Hasegawa, M., Takai, Y., Okumura, Y., Baba, M., Datsenko, K.A., Tomita, M., Wanner, B.L., Mori, H., 2006. Construction of *Escherichia coli* K-12 in-frame, single-gene knockout mutants: the Keio collection (p. 2006 0008). *Mol. Syst. Biol.* 2. <http://dx.doi.org/10.1038/msb4100050>.
- Becart, J., Chevalier, C., Biesse, J., 1990. Quantitative analysis of phospholipids by HPLC with a light-scattering evaporating detector - application to raw materials for cosmetic use. *HRC-J. High. Resolut. Chromatogr.* 13 (2), 126–129.
- Besada-Lombana, P.B., Fernandez-Moya, R., Fenster, J., Silva, N.A. Da, 2017. Engineering *Saccharomyces cerevisiae* fatty acid composition for increased tolerance to octanoic acid. *Biotechnol. Bioeng.* 114 (7), 1531–1538. <http://dx.doi.org/10.1002/bit.26288>.
- Bligh, E.G., Dyer, W.J., 1959. A rapid method of total lipid extraction and purification. *Can. J. Biochem. Physiol.* 37 (8), 911–917.
- Brynildsen, M.P., Liao, J.C., 2009. An integrated network approach identifies the isobutanol response network of *Escherichia coli*. *Mol. Syst. Biol.* 5, 277. <http://dx.doi.org/10.1038/msb.2009.34>.
- Carbon, J., Luna, C.H., 1991. Anionic phospholipids in the control of the membrane-surface potential in *Escherichia coli* - their influence on transport mechanisms. *Int. J. Biochem.* 23 (2), 161–167. [http://dx.doi.org/10.1016/0020-711x\(91\)90184-o](http://dx.doi.org/10.1016/0020-711x(91)90184-o).
- Chen, R., Dou, J., 2016. Biofuels and bio-based chemicals from lignocellulose: metabolic engineering strategies in strain development. *Biotechnol. Lett.* 38 (2), 213–221. <http://dx.doi.org/10.1007/s10529-015-1976-0>.
- Dale, B.E., 2011. Cellulosic biofuels and the road to energy security (9823-9823). *Environ. Sci. Technol.* 45 (23). <http://dx.doi.org/10.1021/es203848y>.
- Datsenko, K.A., Wanner, B.L., 2000. One-step inactivation of chromosomal genes in *Escherichia coli* K-12 using PCR products. *Proc. Natl. Acad. Sci. USA* 97 (12), 6640–6645. <http://dx.doi.org/10.1073/pnas.120163297>.
- Dunlop, M.J., Dossani, Z.Y., Szmids, H.L., Chu, H.C., Lee, T.S., Keasling, J.D., Hadi, M.Z., Mukhopadhyay, A., 2011. Engineering microbial biofuel tolerance and export using efflux pumps (Artn 487). *Mol. Syst. Biol.* 7. <http://dx.doi.org/10.1038/msb.2011.21>.
- Energy, U.D.o., 2016 Billion-Ton Report: Advancing Domestic Resources for a Thriving Bioeconomy, Volume 1: Economic Availability of Feedstocks, B.J.S. M.H. Langholtz, L.M. Eaton (Leads), Editor. 2016: Oak Ridge National Laboratory, Oak Ridge, TN. p. 448.10.2172/1271651.
- Fischer, S., Graber, P., Turina, P., 2000. The activity of the ATP synthase from *Escherichia coli* is regulated by the transmembrane proton motive force. *J. Biol. Chem.* 275 (39), 30157–30162. <http://dx.doi.org/10.1074/jbc.275.39.30157>.
- Fitzgerald, D.J., Stratford, M., Gasson, M.J., Ueckert, J., Bos, A., Narbad, A., 2004. Mode of antimicrobial action of vanillin against *Escherichia coli*, *Lactobacillus plantarum* and *Listeria innocua*. *J. Appl. Microbiol.* 97 (1), 104–113. <http://dx.doi.org/10.1111/j.1365-2672.2004.02275.x>.
- Galanie, S., Thodey, K., Trenchard, I.J., Interrante, M.F., Smolke, C.D., 2015. Synthetic biology complete biosynthesis of opioids in yeast. *Science* 349 (6252), 1095–1100. <http://dx.doi.org/10.1126/science.1259373>.
- Huffer, S., Clark, M.E., Ning, J.C., Blanch, H.W., Clark, D.S., 2011. Role of alcohols in growth, lipid composition, and membrane fluidity of yeasts, bacteria, and archaea. *Appl. Environ. Microbiol.* 77 (18), 6400–6408. <http://dx.doi.org/10.1128/AEM.00694-11>.
- Ingram, L.O., Vreeland, N.S., 1980. Differential effects of ethanol and hexanol on the *Escherichia coli* cell envelope. *J. Bacteriol.* 144 (2), 481–488.
- Inoue, A., Horikoshi, K., 1989. A *Pseudomonas* Thrives in high-concentrations of toluene. *Nature* 338 (6212), 264–266. <http://dx.doi.org/10.1038/338264a0>.
- Jarboe, L.R., Liu, P., Royce, L.A., 2011. Engineering inhibitor tolerance for the production of bio-renewable fuels and chemicals. *Curr. Opin. Chem. Eng.* 1 (1), 38–42. <http://dx.doi.org/10.1016/j.coche.2011.08.003>.
- Jarboe, L.R., Royce, L.A., Liu, P., 2013. Understanding biocatalyst inhibition by carboxylic acids (Artn 272 DOI). *Front. Microbiol.* 4. <http://dx.doi.org/10.3389/fmicb.2013.00272>.
- Jin, T., Rover, M.R., Petersen, E.M., Chi, Z., Smith, R.G., Brown, R.C., Wen, Z., Jarboe, L.R., 2017. Damage to the microbial cell membrane during pyrolytic sugar utilization and strategies for increasing resistance. *J. Ind. Microbiol. Biotechnol.*
- Jo, S., Kim, T., Im, W., 2007. Automated builder and database of protein/membrane complexes for molecular dynamics simulations. *Plos One* 2 (9). <http://dx.doi.org/10.1371/journal.pone.0000880>.
- Jo, S., Kim, T., Iyer, V.G., Im, W., 2008. Software news and updates - CHARNIM-GUI: a web-based graphical user interface for CHARMM. *J. Comput. Chem.* 29 (11), 1859–1865. <http://dx.doi.org/10.1002/jcc.20945>.
- Jo, S., Lim, J.B., Klauda, J.B., Im, W., 2009. CHARMM-GUI membrane builder for mixed bilayers and its application to yeast membranes. *Biophys. J.* 97 (1), 50–58. <http://dx.doi.org/10.1016/j.bpj.2009.04.013>.
- Kakinuma, Y., 1998. Inorganic cation transport and energy transduction in *Enterococcus hirae* and other streptococci. *Microbiol. Mol. Biol. Rev.* 62 (4), 1021–1045.
- Khakbaz, P., Klauda, J.B., 2015. Probing the importance of lipid diversity in cell membranes via molecular simulation. *Chem. Phys. Lipids* 192, 12–22. <http://dx.doi.org/10.1016/j.chemphyslip.2015.08.003>.
- Kircher, M., 2015. Sustainability of biofuels and renewable chemicals production from biomass. *Curr. Opin. Chem. Biol.* 29, 26–31. <http://dx.doi.org/10.1016/j.cbpa.2015.07.010>.
- Klauda, J.B., Venable, R.M., Freites, J.A., O' Connor, J.W., Mondragon-Ramirez, C., Vorobyov, I., Tobias, D.J., MacKerell, A.D., Pastor, R.W., 2010. Update of the CHARMM all-atom additive force field for lipids: Validation on six lipid types. *J. Phys. Chem. B* 114 (23), 7830–7843.
- Konas, R.M., Daristotle, J.L., Harbor, N.B., Klauda, J.B., 2015. Biophysical changes of lipid membranes in the presence of ethanol at varying concentrations. *J. Phys. Chem. B* 119 (41), 13134–13141. <http://dx.doi.org/10.1021/acs.jpcc.5b06066>.
- Korstanje, T.J., van der Vlugt, J.I., Elsevier, C.J., de Bruin, B., 2015. Hydrogenation of carboxylic acids with a homogeneous cobalt catalyst. *Science* 350 (6258), 298–302. <http://dx.doi.org/10.1126/science.1258938>.
- Lam, F.H., Ghaderi, A., Fink, G.R., Stephanopoulos, G., 2014. Biofuels. Engineering alcohol tolerance in yeast. *Science* 346 (6205), 71–75. <http://dx.doi.org/10.1126/science.1257859>.
- Larson, E.D., 2006. A review of life-cycle analysis studies on liquid biofuel systems for the transport sector. *Energy Sustain. Dev.* 10 (2), 109–126. [http://dx.doi.org/10.1016/S0973-0826\(08\)60536-0](http://dx.doi.org/10.1016/S0973-0826(08)60536-0).
- Lennen, R.M., Pfleger, B.F., 2013. Modulating membrane composition alters free fatty acid tolerance in *Escherichia coli* (ARTN e54031). *Plos One* 8 (1). <http://dx.doi.org/10.1371/journal.pone.0054031>.
- Lennen, R.M., Kruziki, M.A., Kumar, K., Zinkel, R.A., Burnum, K.E., Lipton, M.S., Hoover, S.W., Ranatunga, D.R., Wittkopp, T.M., Marner 2nd, W.D., Pfleger, B.F., 2011. Membrane stresses induced by overproduction of free fatty acids in *Escherichia coli*. *Appl. Environ. Microbiol.* 77 (22), 8114–8128. <http://dx.doi.org/10.1128/AEM.05421-11>.
- Lennen, R.M., Politz, M.G., Kruziki, M.A., Pfleger, B.F., 2013. Identification of transport proteins involved in free fatty acid efflux in *Escherichia coli*. *J. Bacteriol.* 195 (1), 135–144. <http://dx.doi.org/10.1128/JB.01477-12>.
- Lian, J., McKenna, R., Rover, M.R., Nielsen, D.R., Wen, Z., Jarboe, L.R., 2016. Production of bio-renewable styrene: utilization of biomass-derived sugars and insights into toxicity. *J. Ind. Microbiol. Biotechnol.*
- Lim, J.B., Klauda, J.B., 2011. Lipid chain branching at the iso- and anteiso-positions in complex chlamydia membranes: a molecular dynamics study. *Biochim. Biophys. Acta-Biomembr.* 1808 (1), 323–331. <http://dx.doi.org/10.1016/j.bbmem.2010.07.036>.
- Liu, P., Chernyshov, A., Najdi, T., Fu, Y., Dickerson, J., Sandmeyer, S., Jarboe, L., 2013. Membrane stress caused by octanoic acid in *Saccharomyces cerevisiae*. *Appl. Microbiol. Biotechnol.* 97 (7), 3239–3251. <http://dx.doi.org/10.1007/s00253-013-4773-5>.
- Lu, J., Tang, J., Liu, Y., Zhu, X., Zhang, T., Zhang, X., 2012. Combinatorial modulation of

- galP and glk gene expression for improved alternative glucose utilization. *Appl. Microbiol Biotechnol.* 93 (6), 2455–2462. <http://dx.doi.org/10.1007/s00253-011-3752-y>.
- Luo, L.H., Seo, P.S., Seo, J.W., Heo, S.Y., Kim, D.H., Kim, C.H., 2009. Improved ethanol tolerance in *Escherichia coli* by changing the cellular fatty acids composition through genetic manipulation. *Biotechnol. Lett.* 31 (12), 1867–1871. <http://dx.doi.org/10.1007/s10529-009-0092-4>.
- McKenna, R., Nielsen, D.R., 2011. Styrene biosynthesis from glucose by engineered *E. coli*. *Metab. Eng.* 13 (5), 544–554. <http://dx.doi.org/10.1016/j.ymben.2011.06.005>.
- Miller, E.N., Jarboe, L.R., Turner, P.C., Pharkya, P., Yomano, L.P., York, S.W., Nunn, D., Shanmugam, K.T., Ingram, L.O., 2009. Furfural inhibits growth by limiting sulfur assimilation in ethanologenic *Escherichia coli* strain LY180. *Appl. Environ. Microbiol.* 75 (19), 6132–6141. <http://dx.doi.org/10.1128/AEM.01187-09>.
- Mills, T.Y., Sandoval, N.R., Gill, R.T., 2009. Cellulosic hydrolysate toxicity and tolerance mechanisms in *Escherichia coli*. *Biotechnol. Biofuels* 2, 26. <http://dx.doi.org/10.1186/1754-6834-2-26>.
- Neidhard, Fc, Bloch, P.L., Smith, D.F., 1974. Culture medium for enterobacteria. *J. Bacteriol.* 119 (3), 736–747.
- Nishibori, A., Kusaka, J., Hara, H., Umeda, M., Matsumoto, K., 2005. Phosphatidylethanolamine domains and localization of phospholipid synthases in *Bacillus subtilis* membranes. *J. Bacteriol.* 187 (6), 2163–2174. <http://dx.doi.org/10.1128/jb.187.6.2163-2174.2005>.
- Oliver, P.M., Crooks, J.A., Leidl, M., Yoon, E.J., Saghatelian, A., Weibel, D.B., 2014. Localization of anionic phospholipids in *Escherichia coli* cells. *J. Bacteriol.* 196 (19), 3386–3398. <http://dx.doi.org/10.1128/JB.01877-14>.
- Pandit, K.R., Klauda, J.B., 2012. Membrane models of *E. coli* containing cyclic moieties in the aliphatic lipid chain. *Biochimica et Biophysica Acta (BBA)-Biomembranes* 1818 (5), 1205–1210.
- Park, J., Rodriguez-Moya, M., Li, M., Pichersky, E., San, K.Y., Gonzalez, R., 2012. Synthesis of methyl ketones by metabolically engineered *Escherichia coli*. *J. Ind. Microbiol Biotechnol.* 39 (11), 1703–1712. <http://dx.doi.org/10.1007/s10029-012-1178-x>.
- Perpina, C., Vinaixa, J., Andreu, C., del Olmo, M., 2015. Development of new tolerant strains to hydrophilic and hydrophobic organic solvents by the yeast surface display methodology. *Appl. Microbiol. Biotechnol.* 99 (2), 775–789. <http://dx.doi.org/10.1007/s00253-014-6048-1>.
- Ramos, J.L., Duque, E., Gallegos, M.T., Godoy, P., Ramos-Gonzalez, M.I., Rojas, A., Teran, W., Segura, A., 2002. Mechanisms of solvent tolerance in gram-negative bacteria. *Annu. Rev. Microbiol.* 56, 743–768. <http://dx.doi.org/10.1146/annurev.micro.56.012302.161038>.
- Roth, B.L., Poot, M., Yue, S.T., Millard, P.J., 1997. Bacterial viability and antibiotic susceptibility testing with SYTOX green nucleic acid stain. *Appl. Environ. Microbiol.* 63 (6), 2421–2431.
- Rowlett, V.W., Mallampalli, V.K.P.S., Karlstaedt, A., Dowhan, W., Taegtmeier, H., Margolin, W., Vitrac, H., 2017. Impact of membrane phospholipid alterations in *Escherichia coli* on cellular function and bacterial stress adaptation. *J. Bacteriol.* 199 (13).
- Royce, L.A., Liu, P., Stebbins, M.J., Hanson, B.C., Jarboe, L.R., 2013. The damaging effects of short chain fatty acids on *Escherichia coli* membranes. *Appl. Microbiol Biotechnol.* 97 (18), 8317–8327. <http://dx.doi.org/10.1007/s00253-013-5113-5>.
- Royce, L.A., Boggess, E., Fu, Y., Liu, P., Shanks, J.V., Dickerson, J., Jarboe, L.R., 2014. Transcriptomic analysis of carboxylic acid challenge in *Escherichia coli*: beyond membrane damage (ARTN e89580). *Plos One* 9 (2). <http://dx.doi.org/10.1371/journal.pone.0089580>.
- Royce, L.A., Yoon, J.M., Chen, Y., Rickenbach, E., Shanks, J.V., Jarboe, L.R., 2015. Evolution for exogenous octanoic acid tolerance improves carboxylic acid production and membrane integrity. *Metab. Eng.* 29, 180–188. <http://dx.doi.org/10.1016/j.ymben.2015.03.014>.
- San, K.-Y., Li, M., Zhang, X., 2011. Bacteria and method for synthesizing fatty acids, Google Patents.
- Sandoval, N.R., Papoutsakis, E.T., 2016. Engineering membrane and cell-wall programs for tolerance to toxic chemicals: beyond solo genes. *Curr. Opin. Microbiol.* 33, 56–66. <http://dx.doi.org/10.1016/j.mib.2016.06.005>.
- Sevin, D.C., Sauer, U., 2014. Ubiquinone accumulation improves osmotic-stress tolerance in *Escherichia coli*. *Nat. Chem. Biol.* 10 (4), 266–272. <http://dx.doi.org/10.1038/nchembio.1437>.
- Sherkhanov, S., Korman, T.P., Bowie, J.U., 2014. Improving the tolerance of *Escherichia coli* to medium-chain fatty acid production. *Metab. Eng.* 25, 1–7. <http://dx.doi.org/10.1016/j.ymben.2014.06.003>.
- Strahl, H., Hamoen, L.W., 2010. Membrane potential is important for bacterial cell division. *Proc. Natl. Acad. Sci. USA* 107 (27), 12281–12286. <http://dx.doi.org/10.1073/pnas.1005485107>.
- Tan, Z., Zhu, X., Chen, J., Li, Q., Zhang, X., 2013. Activating phosphoenolpyruvate carboxylase and phosphoenolpyruvate carboxykinase in combination for improvement of succinate production. *Appl. Environ. Microbiol.* 79 (16), 4838–4844. <http://dx.doi.org/10.1128/aem.00826-13>.
- Tan, Z., Yoon, J.M., Nielsen, D.R., Shanks, J.V., Jarboe, L.R., 2016. Membrane engineering via trans unsaturated fatty acids production improves *Escherichia coli* robustness and production of biorenewables. *Metab. Eng.* <http://dx.doi.org/10.1016/j.ymben.2016.02.004>.
- Trcek, J., Mira, N.P., Jarboe, L.R., 2015. Adaptation and tolerance of bacteria against acetic acid. *Appl. Microbiol. Biotechnol.* 99 (15), 6215–6229. <http://dx.doi.org/10.1007/s00253-015-6762-3>.
- Weber, F.J., de Bont, J.A., 1996. Adaptation mechanisms of microorganisms to the toxic effects of organic solvents on membranes. *Biochim. Biophys. Acta* 1286 (3), 225–245.
- Westman, J.O., Mapelli, V., Taherzadeh, M.J., Franzen, C.J., 2014. Flocculation causes inhibitor tolerance in *Saccharomyces cerevisiae* for second-generation bioethanol production. *Appl. Environ. Microbiol.* 80 (22), 6908–6918. <http://dx.doi.org/10.1128/aem.01906-14>.
- Wu, E.L., Cheng, X., Jo, S., Rui, H., Song, K.C., Davila-Contreras, E.M., Qi, Y.F., Lee, J.M., Monje-Galvan, V., Venable, R.M., Klauda, J.B., Im, W., 2014. CHARMM-GUI membrane builder toward realistic biological membrane simulations. *J. Comput. Chem.* 35 (27), 1997–2004. <http://dx.doi.org/10.1002/jcc.23702>.
- Zaldivar, J., Ingram, L.O., 1999. Effect of organic acids on the growth and fermentation of ethanologenic *Escherichia coli* LY01. *Biotechnol. Bioeng.* 66 (4), 203–210.
- Zaldivar, J., Martinez, A., Ingram, L.O., 1999. Effect of selected aldehydes on the growth and fermentation of ethanologenic *Escherichia coli*. *Biotechnol. Bioeng.* 65 (1), 24–33.
- Zhang, X., Jantama, K., Moore, J.C., Jarboe, L.R., Shanmugam, K.T., Ingram, L.O., 2009. Metabolic evolution of energy-conserving pathways for succinate production in *Escherichia coli*. *Proc. Natl. Acad. Sci. USA* 106 (48), 20180–20185. <http://dx.doi.org/10.1073/pnas.0905396106>.
- Zhu, X., Tan, Z., Xu, H., Chen, J., Tang, J., Zhang, X., 2014. Metabolic evolution of two reducing equivalent-conserving pathways for high-yield succinate production in *Escherichia coli*. *Metab. Eng.* 24C, 87–96. <http://dx.doi.org/10.1016/j.ymben.2014.05.003>.